

# Distributed Balanced Photodetectors for Broad-Band Noise Suppression

M. Saiful Islam, *Student Member*, Tai Chau, *Student Member*, Sagi Mathai, *Student Member*, Tatsuo Itoh, *Life Fellow*, Ming C. Wu, *Member, IEEE*, Deborah L. Sivco, and Alfred Y. Cho, *Fellow, IEEE*

**Abstract**—A novel velocity-matched distributed balanced photodetector with a 50- $\Omega$  coplanar waveguide output transmission line has been experimentally demonstrated in the InP/InGaAs material system. Distributed absorption and velocity matching are employed to increase the saturation photocurrent. A common-mode rejection ratio greater than 27 dB has been achieved. The radio-frequency (RF) link experiment conducted at 4.16 GHz shows that the relative intensity noise of the laser has been suppressed by more than 24 dB and shot-noise limited performance has been achieved. Significant improvement of signal-to-noise ratio has been observed over a wide range of frequencies and phase mismatch of input RF signals.

**Index Terms**—Analog fiber-optic links, balanced photodetectors, microwave photonics, noise suppression, optical receivers, RF photonics.

## I. INTRODUCTION

BALANCED photodetectors (PD's) play a very important role in a high-performance radio-frequency (RF) photonic system because they can suppress laser relative intensity noise (RIN) and amplified spontaneous emission noise (ASE) from erbium-doped fiber amplifiers (EDFA's) [1]. When used in conjunction with an external modulator with complementary outputs, shot noise-limited system performance can be achieved. We can continue to improve the noise figure and spurious-free dynamic range (SFDR) of externally modulated links by increasing the power of the optical carrier. Therefore, balanced PD's with broad bandwidth and high-saturation photocurrents are particularly important for analog fiber-optic-link applications. Though discrete balanced PD's with high-saturation power have been reported, their bandwidth is limited [2]. Monolithically integrated balanced PD's offer superior performance (broader bandwidth, better matching of photodiodes) and reduced packaging cost. However, most of the reported integrated balanced receivers suffer from low-saturation power and are not suitable for analog links [3]–[5].

There have been several publications aimed at simultaneously achieving high power and high bandwidths in PD's using waveguide [6], traveling wave [7], and traveling-wave-

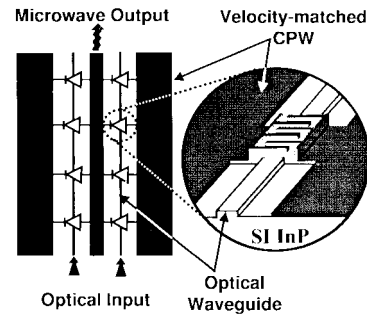


Fig. 1. Principle and schematic structure of the distributed balanced PD. The inset shows the active region with an MSM photodiode.

hybrid detector arrays [8]. Previously, we have reported a velocity-matched distributed photodetector (VMDP) with a peak saturation photocurrent of 56 mA and a 3-dB bandwidth of 49 GHz [9]. Recently, an InP-based long wavelength VMDP has also been reported [10]. Compared with other PD structures, the VMDP is more suitable for implementing balanced photodetection since it has separate optical and microwave waveguides. In this paper, we propose and demonstrate a novel monolithic distributed balanced PD that can simultaneously achieve high-saturation photocurrent and large bandwidth. A common-mode rejection ratio (CMRR) of 27 dB and a noise suppression of 24 dB have been experimentally demonstrated.

## II. DESIGN AND FABRICATION

Fig. 1 depicts the principle and schematic structure of the distributed balanced PD, which consists of two input optical waveguides, two arrays of high-speed metal–semiconductor–metal (MSM) photodiodes distributed along the optical waveguides, and a 50- $\Omega$  coplanar waveguide (CPW) output transmission line. The detector operates in balanced mode when a voltage bias is applied between the two ground electrodes of the CPW. The common-mode photocurrent flows directly to the bottom ground electrode, while the difference photocurrent (signal) flows to the center conductor. The signal is then collected by the CPW. The diodes are 23- $\mu\text{m}$ -long and 5- $\mu\text{m}$  wide. The separation between photodiodes is 150  $\mu\text{m}$ . The MSM fingers with 1- $\mu\text{m}$  width and 1- $\mu\text{m}$  spacing are patterned by optical lithography. The overlap of the MSM fingers is 10.5  $\mu\text{m}$ . The central conductor of the CPW has a width of 55  $\mu\text{m}$ , and the separation between the central conductor and the ground conductors is 85  $\mu\text{m}$ . Without the photodiodes, the velocity of the CPW is about 31.8% faster than the light

Manuscript received October 4, 1998; revised March 15, 1999. This work was supported in part by the Office of Naval Research Multi University Research Initiative (MURI) on RF Photonics, by the National Radio Astronomy Observatory (NRAO), and by the University of California Microelectronics Innovation and Computer Research Opportunities (UC MICRO).

M. S. Islam, T. Chau, S. Mathai, T. Itoh, and M. C. Wu are with the Electrical Engineering Department, University of California at Los Angeles, Los Angeles, CA 90095-1594 USA (e-mail: wu@ee.ucla.edu).

D. L. Sivco and A. Y. Cho are with Lucent Technologies, Bell Laboratories, Murray Hill, NJ 07974 USA.

Publisher Item Identifier S 0018-9480(99)05197-2.

velocity in the optical waveguide. The photodiode arrays provide periodic capacitance loading to slow down the microwave velocity. By adjusting the length and separation of photodiodes, velocity matching between the CPW and optical waveguides is achieved. The impedance of the CPW is also matched to  $50\ \Omega$ .

We designed the distributed balanced PD to inherit the basic advantages of the VMDP, namely, high-saturation photocurrent, high quantum efficiency, and large bandwidth. Although only the difference current (ac signal) is collected in the balanced PD, the PD's still have to absorb the dc light. As a result, high dc saturation photocurrent is required for the distributed balanced PD's. The photodiodes are designed to operate below saturation under high optical input by coupling only a small fraction of light from the passive waveguide to each individual photodiode. Though longer absorption length is required in order to attain high power, the bandwidth of the distributed balanced PD remains high because of velocity matching. The linearity of the detector is also improved by distributed absorption because the photo-generated carrier density is reduced in the active region. Though MSM photodiodes are used in our experiment, the concept presented in this paper is applicable to distributed balanced PD's using p-i-n or other vertical transport PD's whose linearity is inherently better due to their uniform electric field distribution.

#### A. Optical Waveguide

The optical waveguide consists of the following: a 200-nm-thick  $\text{In}_{0.52}\text{Al}_{0.37}\text{Ga}_{0.11}\text{As}$  lower cladding layer, a 500-nm-thick  $\text{In}_{0.52}\text{Al}_{0.178}\text{Ga}_{0.302}\text{As}$  core region, a 200-nm-thick  $\text{In}_{0.52}\text{Al}_{0.37}\text{Ga}_{0.11}\text{As}$  first upper cladding layer, and a thin  $\text{In}_{0.52}\text{Al}_{0.48}\text{As}$  second upper cladding layer. The 150-nm-thick absorption region is located on top of the waveguide for evanescent coupling. Since the Schottky barrier height of most metals on InGaAs is typically between 0.2–0.3 eV, an  $\text{In}_{0.52}\text{Al}_{0.48}\text{As}$  cap layer is used to increase the Schottky barrier height and, therefore, reduce the dark current of the photodiodes [11]. A graded layer is incorporated in the structure to reduce the minority carrier trapping at the InAlAs-InGaAs band edge discontinuity. A scalar three-dimensional beam propagation method (BPM) was used to simulate the optical properties of the balanced VMDP. Since the two optical waveguides are  $140\ \mu\text{m}$  apart, no optical coupling between the waveguides is expected. This is also confirmed by the BPM simulation.

#### B. Modeling of Microwave Transmission Line

The impedance and the phase velocity of the CPW are calculated using the equivalent-circuit model described in [12]. The length of the photodiodes and the separation between them are adjusted to achieve simultaneous velocity matching and impedance matching. Since the separation between the central conductor and the ground electrodes ( $85\ \mu\text{m}$ ) are much smaller than the wavelength of the RF signal (about two orders of magnitude smaller at 50 GHz), quasi-static analysis is reasonably accurate [13]. The capacitors and resistors of each photodiode are considered lumped elements in our quasi-static simulation. After optimizing the receiver structure, a full-wave

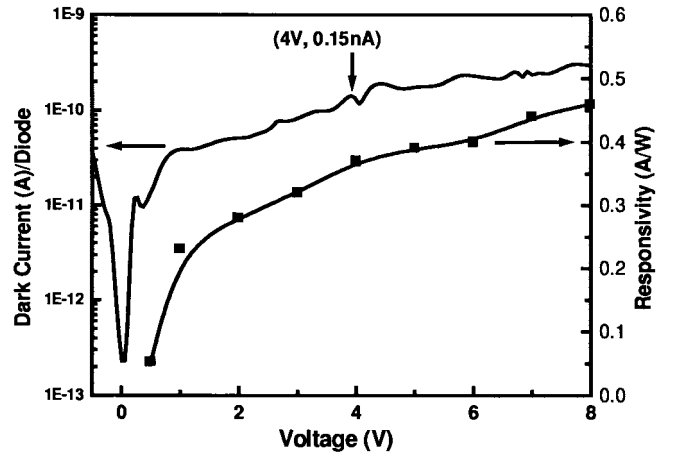


Fig. 2. The dark current (left) and dc responsivity (right) versus bias voltage for individual VMDP (one array of photodiodes) in the balanced detector. At the operational bias (4 V), the dark current is 0.15 nA.

analysis was performed to verify the design. We found that the quasi-static results agree very well with the full-wave analysis for frequencies below 100 GHz. The period in our device corresponds to a cutoff frequency of 300 GHz, well above our expected frequency of operation. Therefore, the dispersion due to the periodicity of the structure is negligible for frequencies below 100 GHz [14].

By etching the InGaAs layer, except in the active areas of the photodiodes, the mesas were patterned on the wafer structure. Ridge waveguides with 100-nm ridge height were formed by wet chemical etching. The active regions of the photodiodes were defined by opening  $6 \times 23\text{-}\mu\text{m}^2$  windows on a 150-nm-thick silicon-nitride ( $\text{Si}_3\text{N}_4$ ) film deposited by plasma-enhanced chemical vapor deposition (PECVD). Buffered HF was used to open the windows. The Ti-Au electrodes and contact pads were then delineated by standard lift-off process. The tips of the MSM fingers are placed on top of the  $\text{Si}_3\text{N}_4$  to suppress soft breakdown and enable the MSM diodes to operate over a wider range of bias voltages [16]. A thick CPW was formed by standard liftoff process to connect the distributed balanced PD's. Finally, the balanced detector structure is lapped down to  $150\ \mu\text{m}$ , cleaved, and mounted on copper heat sinks. By measuring the forward current-voltage characteristics, the barrier height of the metal-semiconductor junction was estimated to be 0.57 eV.

### III. EXPERIMENTAL RESULTS

The balanced VMDP exhibits very good electrical and optical characteristics. The dark current is measured to be  $28\ \mu\text{A}/\text{cm}^2$  at 10 V bias, the lowest reported for InAlAs/InGaAs MSM photodiodes (Fig. 2). At an operating voltage of 4 V, the total dark current of a balanced receiver with five pairs of photodiodes is 1.5 nA. We used a pair of lensed fibers to couple light into the PD. Fig. 2 also shows the measured dc responsivity of the PD as a function of bias voltage. The average dc responsivity was measured to be 0.45 A/W at 8-V bias. Responsivity as high as 0.6 A/W has been observed in some devices. The photo response to a laser beam with TM polarization is measured to be  $\sim 1.7\ \text{dB}$  higher than that of TE polarization. With antireflection coating, the average

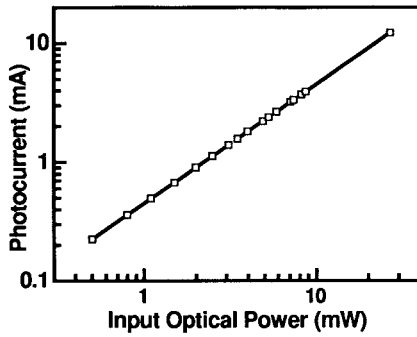


Fig. 3. DC photocurrent versus input optical power (without antireflection coating). The dc photocurrent remains linear up to 12 mA.

responsivity can be increased to 0.64 A/W. The responsivity can be further improved by optimizing the coupling efficiency of the lensed fiber, as well as reducing the coupling loss between the passive and active waveguide regions by better control of the etching steps during fabrication.

At 8 V, bias of the dc photocurrent is linear up to 12 mA on each branch of the receiver (Fig. 3). Nonlinearity is observed at higher photocurrent. At 19 mA of photocurrent, degradation of dark current is observed. The damage was mainly caused by localized high temperature in the device active region [16]. Detailed analysis of our current structure shows that significant optical scattering loss occurs at the transition between the passive optical waveguide and active photodiode region due to the large discontinuity in waveguide and active region mesa width. We are currently working on a VM DP with uniform waveguide and active-region mesa width to reduce the scattering loss and achieve more uniform distribution of photocurrent.

An HP 8510C network analyzer was used to measure the microwave characteristics of the balanced receiver without input light. The device used for microwave measurement had a length of 2 mm with 12 pairs of photodiodes. Detailed measurement results have been presented in [17]. The measured characteristic impedance of the receiver is 50  $\Omega$  with a variation of less than 3%. The  $S_{11}$ -parameter is below -30 dB from 45 MHz to 40 GHz. The  $S_{12}$ -parameter shows a maximum drop of only 0.6 dB in the same frequency range, indicating that the attenuation of the photocurrent will be less than 0.6 dB since it is generated inside the structure.

The frequency response of the receiver was measured by coupling light to only one waveguide at a time. Fig. 4 shows the frequency response of the PD. Using the optical heterodyne technique with two external-cavity tunable semiconductor lasers at 1.55  $\mu\text{m}$ , the 3-dB bandwidth was found to be 16 GHz for both PD arrays. The bandwidth is currently limited by the carrier transit time of the MSM photodiodes. Since the bandwidth of our capacitance loaded CPW is much greater than 40 GHz, the bandwidth of the balanced VM DP can be increased by scaling down the MSM photodiodes.

The experimental setup for balanced detection is shown in Fig. 5. A distributed feedback (DFB) laser with 1542-nm wavelength and 0-dBm output power is employed as the optical source. It is amplified by an EDFA and then filtered by an optical bandpass filter with 2-nm bandwidth. The microwave signal was modulated onto the optical carrier by an

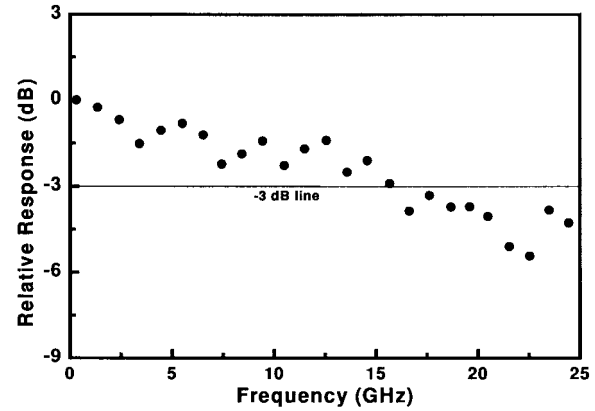


Fig. 4. Frequency response of the distributed balanced PD illuminating only one waveguide at a time.

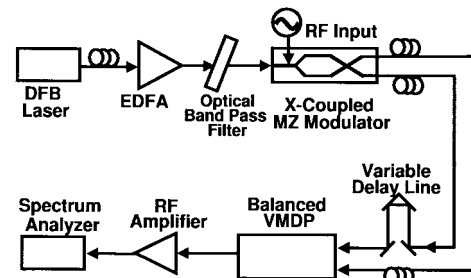


Fig. 5. Experimental setup for balanced detection. The complimentary input signals are produced by the X-coupled MZ modulator.

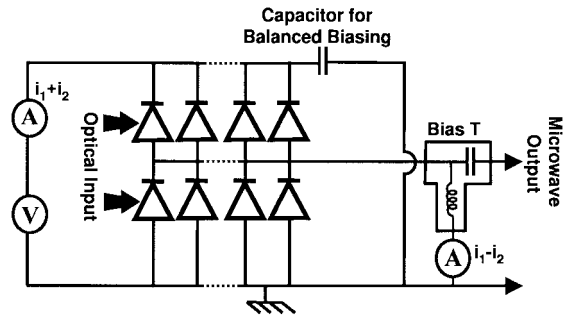


Fig. 6. The biasing circuit for balanced detection.

X-coupled Mach-Zehnder modulator (MZM), which produces two complimentary outputs. The outputs are coupled to the balanced VM DP by two lensed fibers. To maximize the signal enhancement and noise cancellation, it is important to match the amplitudes and phases of the two detected microwave signals. In our experiment, a variable attenuator was used to match the amplitudes of the photocurrents. Typical balance was within 2% of the balanced VM DP total photocurrent. We also employed a variable optical delay line to match the fiber lengths from the MZM to the balanced receiver to ensure 180° phase difference in the RF signals.

Balanced detection is achieved by applying a bias of 8 V between the two ground electrodes of the CPW. A custom-made high-frequency probe with an integrated dc-blocking capacitor on one ground probe is used to collect the microwave output signal. Fig. 6 shows the biasing scheme. We verified balanced detection by tuning a delay line [17]. We obtained an

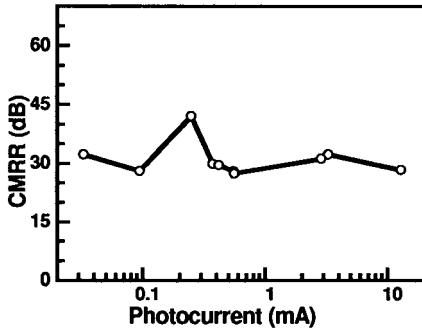


Fig. 7. CMRR versus photocurrent for the distributed balanced receiver. The high CMRR results from the closely matched photodiode characteristics in our monolithic device.

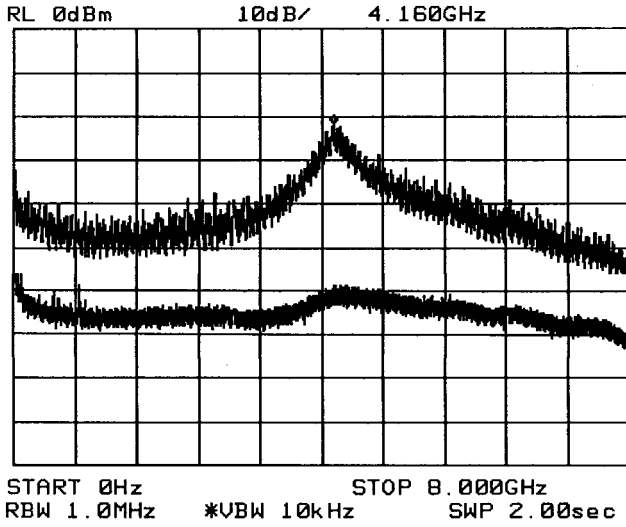


Fig. 8. The noise spectra of a DFB laser measured by the distributed balanced PD in unbalanced mode (top trace) and balanced mode (bottom trace). Other than some frequencies where RIN is very high, the receiver suppresses noise below the shot noise floor. Measurements are done with a photocurrent of 4.2 mA.

extinction ratio of more than 44 dB between phase difference of  $0^\circ$  and  $180^\circ$ .

We measured the dc photocurrents with two current monitors (Keithley Picoammeter): the difference photocurrent ( $i_{\text{DIFF}}$ ) is monitored through the bias-T connected to the probe, and the common-mode photocurrent ( $i_{\text{COM}}$ ) is monitored between the ground electrodes of the CPW. Fig. 7 shows the CMRR, defined as  $\text{CMRR} = 20 \cdot \log(i_{\text{COM}}/i_{\text{DIFF}})$ , as a function of the total photocurrent. Very high CMRR ( $>27$  dB) is measured for a wide range of photocurrent from 30 nA to 12 mA. Similar magnitude of CMRR was also measured for a wide frequency range. This is attributed to the well-matched characteristics of the photodiodes in our monolithic balanced detectors.

One key advantage of the balanced PD is its ability to cancel out the laser RIN. To evaluate the cancellation ratio of our device, we compare the noise spectra of a DFB laser measured by our PD in the unbalanced and balanced modes. The DFB laser operates in continuous wave (CW) condition and has a RIN peak at 4.16 GHz. The top trace in Fig. 8 shows the noise spectra measured near its RIN peak when only one waveguide

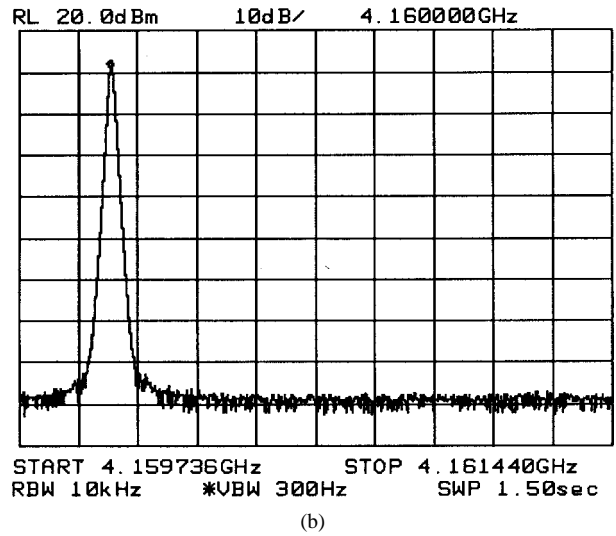
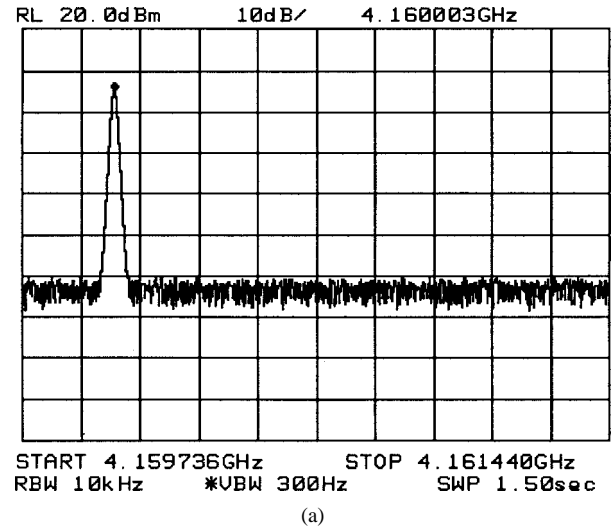


Fig. 9. The RF spectra of the modulated signal detected in (a) unbalanced and (b) balanced modes. The peak of the balanced output is 6 dB higher than that of the unbalanced signal. Noise suppression in excess of 24 dB is achieved.

is illuminated. We confirm that the noise is dominated by the RIN of the DFB laser. When the optical input power is doubled, the noise floor increases by 6 dB. We then biased the PD in the balanced mode and coupled the input to both the optical waveguides. The bottom trace in Fig. 8 shows the noise spectra detected by the balanced detector. Suppression of RIN by as much as 36 dB is observed at the frequencies of highest RIN. Due to equal fiber lengths for both inputs, uniform noise cancellation is achieved for all the frequencies.

Fig. 9 shows the RF spectra of the output from the balanced VMDP in the unbalanced (only one waveguide is illuminated) and balanced mode. Suppression of the noise floor by 24 dB has been achieved in the balanced mode. The signal is also enhanced by 6 dB. Different magnitudes of noise suppression were observed over a wide frequency range up to 11 GHz. Fig. 10 plots the total amount of noise cancelled versus frequency. For the upper curve, the DFB was biased at 23.1 mA and was found to have very high RIN noise (shown in Fig. 8). The lower curve is for a bias of 31-mA current. In both

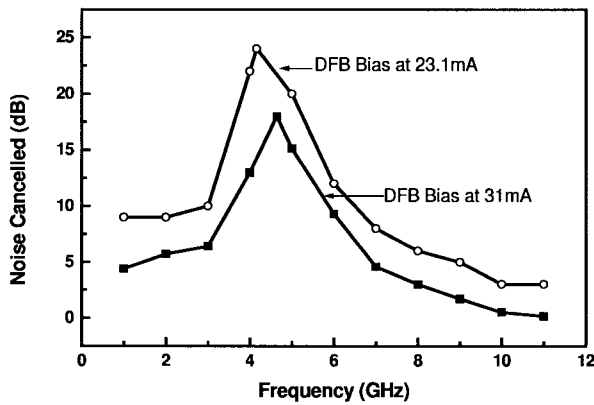


Fig. 10. The total amount of suppressed noise at different frequencies is plotted for two different DFB bias currents. In both cases, RIN is suppressed below the shot noise floor.

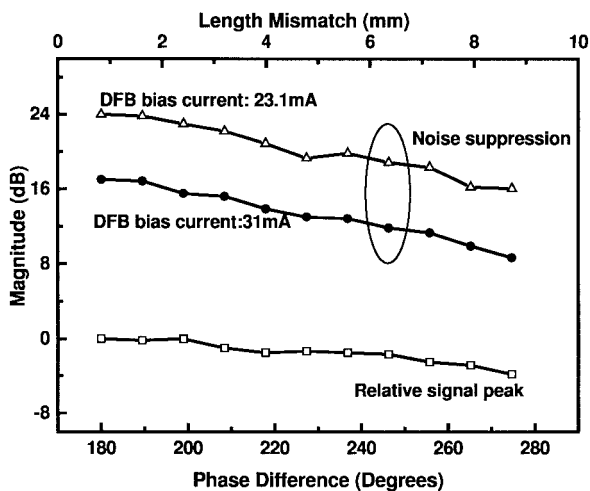


Fig. 11. Total amount of noise suppression and the deviation of the signal peak versus phase deviation of the RF signal from  $180^\circ$ . Even with a phase variation of  $100^\circ$ , the receiver can suppress more than 16 dB of RIN noise, whereas the signal peak reduction is less than 4 dB.

cases, the receiver reaches the shot noise floor by canceling the RIN in the carrier.

The RF signals detected by the balanced detector should be exactly at  $180^\circ$  out of phase for optimum noise suppression. This requires the lengths of the fiber from the complimentary MZM to the detector to be exactly the same in length. In practical applications, the optical path length will drift slightly due to environmental changes, and it is important to understand the impact of phase mismatch. Fig. 11 plots the variation in the signal peak and the amount of noise suppression when the phase difference of the RF signals deviates from  $180^\circ$  due to fiber length mismatch in the link. Even with a phase variation of  $100^\circ$ , the receiver can suppress more than 16 dB of RIN noise, whereas the signal peak reduction is less than 4 dB. For a 8-GHz signal, this mismatch corresponds to 8.5 mm of fiber length.

By fixing the RF carrier at 6.5 GHz, we measured the signal-to-noise-ratio (SNR) of the link versus the received optical power for both the distributed balanced receiver and a reference receiver with a single detector. The SNR for the single detector receiver is almost constant with increasing optical power, indicating that the receiver noise is dominated

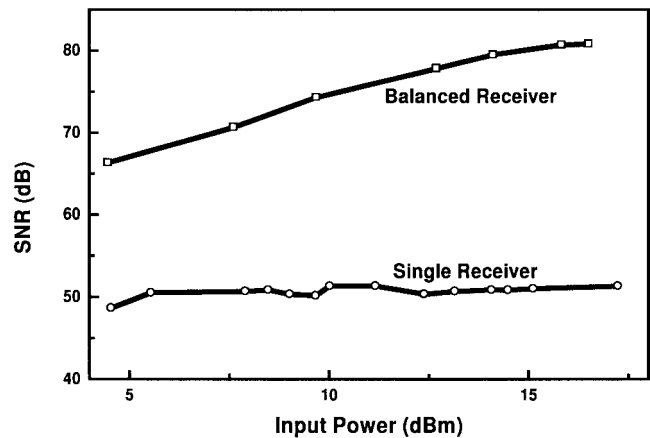


Fig. 12. Measured SNR of the balanced receiver. The lower curve shows the SNR for the receiver in an unbalanced configuration.

by the RIN (Fig. 12). In contrast, the SNR for the balanced receiver increases monotonically with optical power up to 15 dBm. For optical power greater than 15 dBm, the SNR still increases monotonically with optical power at a smaller rate. This suggests the presence of some residual RIN. Comparing the two receivers, it is also noted that the SNR for the balanced receiver is 23 dB higher than the single detector receiver.

#### IV. CONCLUSION

We have successfully designed, fabricated, and experimentally demonstrated a balanced VMDP with both impedance and velocity matching. The device exhibits a very low dark current (1.5 nA for the balanced VMDP with five pairs of photodiodes) and a high external quantum efficiency (0.60 A/W). The RIN of a semiconductor distributed feedback laser has been suppressed by 24 dB, and the RF signal has been enhanced by 6 dB. Significant improvement in SNR has been observed over a broad frequency range. The experimental results indicate that the distributed balanced PD will have a major impact on most RF photonic systems.

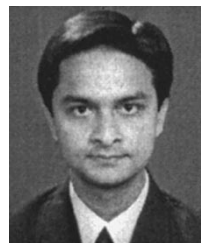
#### ACKNOWLEDGMENT

The authors acknowledge Dr. D. T. K. Tong, Lucent Technologies, Bell Laboratories, Holmdel, NJ, for his helpful suggestion about the experimental setup, and W. R. Deal and T. Jung, University of California at Los Angeles, for their helpful discussion about the measurements.

#### REFERENCES

- [1] L. T. Nichols, K. J. Williams, and R. D. Esman, "Optimizing the ultrawide-band photonic link," *IEEE Trans. Microwave Theory Tech.*, vol. 45, pp. 1384–1389, Aug. 1997.
- [2] K. J. Williams and R. D. Esman, "Optically amplified down converting link with shot-noise limited performance," *IEEE Photon. Technol. Lett.*, vol. 8, pp. 148–150, Jan. 1996.
- [3] D. Trommer, A. Umbach, W. Passenberg, and G. Unterborsch, "A monolithically integrated balanced mixer OEIC on InP for coherent receiver applications," *IEEE Photon. Technol. Lett.*, vol. 5, pp. 1038–1040, Sept. 1993.
- [4] F. Ghirardi, A. Bruno, B. Mersali, J. Brandon, L. Giraudet, A. Scavennec, and A. Carencu, "Monolithic integration of an InP based polarization diversity heterodyne photoreceiver with electrooptic adjustability," *J. Lightwave Technol.*, vol. 13, pp. 1536–1549, July 1995.

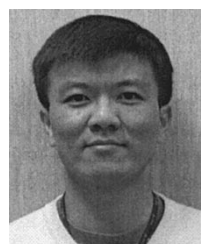
- [5] R. J. Deri, E. C. M. Pennings, A. Scherer, A. S. Gozdz, C. Caneau, N. C. Andreadakis, V. Shah, L. Curtis, R. J. Hawkins, J. B. D. Soole, and J. I. Song, "Ultracompact monolithic integration of balanced, polarization diversity photodetectors for coherent lightwave receivers," *IEEE Photon. Technol. Lett.*, vol. 4, pp. 1238–1240, Nov. 1992.
- [6] S. Jasmin, N. Vojdani, J. C. Renaud, and A. Enard, "Diluted and distributed-absorption microwave waveguide photodiodes for high efficiency and high power," *IEEE Trans. Microwave Theory Tech.*, vol. 45, pp. 1337–1341, Aug. 1997.
- [7] K. S. Giboney, M. J. W. Rodwell, and J. E. Bowers, "Travelling-wave photodetector theory," *IEEE Trans. Microwave Theory Tech.*, vol. 45, pp. 1310–1319, Aug. 1997.
- [8] C. L. Goldsmith, G. A. Magel, and R. J. Boca, "Principals and performance of travelling-wave photodetector arrays," *IEEE Trans. Microwave Theory Tech.*, vol. 45, pp. 1310–1319, Aug. 1997.
- [9] L. Y. Lin, M. C. Wu, T. Itoh, T. A. Vang, R. E. Muller, D. L. Sivco, and A. Y. Cho, "Velocity-matched distributed photodetectors with high-saturation power and large bandwidth," *IEEE Photon. Technol. Lett.*, vol. 8, pp. 1376–1378, Oct. 1996.
- [10] T. Chau, L. Fan, D. T. K. Tong, S. Mathai, M. C. Wu, D. L. Sivco, and A. Y. Cho, "Long wavelength velocity-matched distributed photodetectors for RF fiber optic links," *Electron. Lett.*, vol. 34, no. 14, pp. 1422–1424, July 1998.
- [11] E. Sano, M. Yoneama, T. Enoki, and T. Tamamura, "Performance dependence of InGaAs MSM photodetectors on barrier-enhancement layer structures," *Electron. Lett.*, vol. 28, no. 13, pp. 1220–1221, 1992.
- [12] L. Y. Lin, M. C. Wu, T. Itoh, T. A. Vang, R. E. Muller, D. L. Sivco, and A. Y. Cho, "High-power high-speed photodetectors-design, analysis and experimental demonstration," *IEEE Trans. Microwave Theory Tech.*, vol. 45, pp. 1320–1331, Aug. 1997.
- [13] M. N. Khan, A. Gopinath, J. P. G. Bristow, and J. P. Donnelly, "Technique for velocity-matching traveling-wave electrooptic modulator in AlGaAs/GaAs," *IEEE Trans. Microwave Theory Tech.*, vol. 41, pp. 244–249, Feb. 1993.
- [14] R. Spickermann and N. Dagli, "Experimental analysis of millimeter wave coplanar waveguide slow wave structure on GaAs," *IEEE Trans. Microwave Theory Tech.*, vol. 42, pp. 1918–1924, Oct. 1994.
- [15] W. A. Wohlmuth, P. Fay, and I. Adesida, "Dark current suppression in GaAs metal-semiconductor-metal photodetectors," *IEEE Photon. Technol. Lett.*, vol. 8, pp. 1061–1064, Aug. 1996.
- [16] A. Nespola, T. Chau, M. Pirola, M. C. Wu, G. Ghione, and C. U. Naldi, "Failure analysis of travelling wave MSM distributed photodetectors," in *Int. Electron. Devices Meeting*, San Francisco, CA, Dec. 6–9, 1998.
- [17] M. S. Islam, T. Chau, S. Mathai, A. Rollinger, A. Nespola, W. R. Deal, T. Itoh, and M. C. Wu, "Distributed balanced photodetectors for RF photonic links," in *Int. Topical Meeting Microwave Photon.*, Princeton, NJ, Oct. 12–14, 1998.



**M. Saiful Islam** (S'98) received the B.Sc. degree in physics from the Middle East Technical University, Ankara, Turkey, in 1994, the M.Sc. degree in physics from Bilkent University, Ankara, Turkey, in 1996, the M.S. degree in electrical engineering from the University of California at Los Angeles (UCLA), in 1998, and is currently working toward the Ph.D. degree at UCLA.

His research interests include design, fabrication, and characterization of ultra-fast resonant cavity enhanced PD's, high-power and high-efficiency PD's, distributed balanced photoreceivers, and their system application in high-performance fiber-optic links.

Mr. Islam is a member of the American Physical Society.



**Tai Chau** (S'97) received the B.S. and M.S. degrees in electrical engineering from the University of California at Los Angeles (UCLA), in 1994 and 1996, respectively, and is currently working toward the Ph.D. degree at UCLA.

His main research interests include integrated microwave photonic devices and high-power high-speed traveling-wave PD's.



**Sagi Mathai** (S'97) received the B.S. degree in electrical engineering from the University of California at Los Angeles (UCLA), in 1997, and is currently working toward the M.S. and Ph.D. degrees in electrical engineering from UCLA.

His research interests have included velocity-matched distributed PD's (VMPD's) and distributed balanced photoreceivers. His current research interest includes traveling-wave electroabsorption modulators and its applications in fiber-optic links.

Mr. Mathai is a member of Eta Kappa Nu.



**Tatsuo Itoh** (S'69–M'69–SM'74–F'82–LF'94) received the Ph.D. degree in electrical engineering from the University of Illinois at Urbana-Champaign, in 1969.

From September 1966 to April 1976, he was with the Electrical Engineering Department, University of Illinois at Urbana-Champaign. From April 1976 to August 1977, he was a Senior Research Engineer in the Radio Physics Laboratory, SRI International, Menlo Park, CA. From August 1977 to June 1978, he was an Associate Professor at the University of Kentucky, Lexington. In July 1978, he joined the faculty at the University of Texas at Austin, where he became a Professor of electrical engineering in 1981 and Director of the Electrical Engineering Research Laboratory in 1984. During the summer of 1979, he was a Guest Researcher at AEB-Telefunken, Ulm, Germany. In September 1983, he was selected to hold the Hayden head Centennial Professorship of Engineering at the University of Texas. In September 1984, he was appointed Associate Chairman for Research and Planning, Electrical, and Computer Engineering Department, University of Texas. In January 1991, he joined the University of California at Los Angeles, as Professor of electrical engineering and Holder of the TRW Endowed Chair in Microwave and Millimeter Wave Electronics. He was an Honorary Visiting Professor at Nanjing Institute of Technology, China, and at Japan Defense Academy. He is currently Director of Joint Services, Electronics Program (JSEP) and Director of the Multidisciplinary University Research Initiative (MURI) Program at the University of California at Los Angeles (UCLA). In April 1994, he was appointed as Adjunct Research Officer for the Communications Research Laboratory, Ministry of Post and Telecommunication, Japan. He currently holds a Visiting Professorship at the University of Leeds, U.K., and is an External Examiner of the Graduate Program of the City University of Hong Kong. He has authored or co-authored over 245 journal publications, 470 refereed conference presentations, and has written over 26 books and book chapter in the area of microwave, millimeter-wave, antennas, and numerical electromagnetics. He has also produced 40 Ph.D. students. He was the chairman of USNC/URSI Commission D from 1988 to 1990, the vice chairman of Commission D of the International URSI from 1991 to 1993, and chairman from 1993 to 1996. He is on the Long Range Planning Committee of URSI. He serves on advisory boards and committees of a number of organizations, including the National Research Council and the Institute of Mobile and Satellite Communication, Germany.

Dr. Itoh is a member of the Institute of Electronics and Communication Engineers, Japan, Commissions B and D of USNC/URSI, and was elected honorary life member of the IEEE Microwave Theory and Techniques Society, in 1994. He serves on the Administrative Committee of the IEEE Microwave Theory and Techniques Society. He served as Editor-in-Chief of the IEEE TRANSACTIONS ON MICROWAVE THEORY AND TECHNIQUES from 1983 to 1985. He was vice president of the IEEE Microwave Theory and Techniques Society in 1989 and was president in 1990. He was the editor-in-chief of the IEEE MICROWAVE AND GUIDED WAVE LETTERS from 1991 to 1994. He has been the recipient of a number of awards, including the Shida Award presented by the Japanese Ministry of Post and Telecommunications in 1998, and the Japan Microwave Prize in 1998.



**Deborah L. Sivco** received the B.A. degree in chemistry from Rutgers University, New Brunswick, NJ, in 1980, and the M.S. degree in materials Science from Steven Institute of Technology, Hoboken, NJ, in 1988.

In 1981, she joined Bell Laboratories, and is currently a Member of Technical Staff in the Semiconductor Research Laboratory, Bell Laboratories, Lucent Technologies, Murray Hill, NJ. She has been involved with molecular beam epitaxial (MBE) growth of III-V compounds since 1981. She has performed the crystal growth of GaAs/AlGaAs and InGaAs/InAlAs heterostructures for field-effect transistors, resonant tunneling transistors, bipolar transistors, double heterostructure lasers, and detectors. She recently prepared the world's first quantum cascade laser, designed by Faist *et al.*, using bandgap engineering. She has co-authored 170 journal papers and holds nine patents.

Ms. Sivco was co-recipient of the Newcomb Cleveland Prize, AAAS 1994, the *British Electronics Letters* Premium Award, 1995, and a 1996 Technology of the Year Award from *Industry Week* magazine.



**Alfred Y. Cho** (S'57-M'60-SM'79-F'81) was born in Beijing, China. He received the B.S., M.Sc., and Ph.D. in electrical engineering from the University of Illinois at Urbana-Champaign.

In 1968, he joined Bell Laboratories, as a Member of Technical Staff, and was promoted to Department Head in 1984. He was Director of the Materials Processing Research Laboratory in 1987 and, in 1990, became Director of Semiconductor Research. His pioneering work on molecular beam epitaxy (MBE) has had a significant impact on the semiconductor industry, leading to the making of faster and more efficient electronic and opto-electronic semiconductor devices.

Dr. Cho is a member of the Chinese Academy of Sciences, Academia Sinica, Third World Academy of Sciences, American Academy of Arts and Sciences, National Academy of Engineering, National Academy of Sciences, and the American Philosophical Society. He is the recipient of numerous award from technical and professional societies. These awards include the 1982 International Prize for New Materials from the American Physical Society, the 1987 Solid State Science and Technology Medal of the Electrochemical Society, the 1988 World Materials Congress of ASM International Award, the 1990 International Crystal Growth Award of the American Association for Crystal Growth, the 1993 National Medal of Science, presented by President Clinton, the 1994 IEEE Medal of Honor, the 1995 Elliott Cresson Medal of the Franklin Institute, the 1995 C & C (Computer and Communications) Prize, and Japan and the New Jersey Inventors Hall of Fame, 1997.